






ORIGINAL ARTICLE

Intramuscular cabotegravir and rilpivirine concentrations after switching from efavirenz-containing regimen

Sara Bettonte^{1,2}  | Mattia Berton^{1,2}  | Felix Stader³  | Manuel Battegay^{1,2}  |
Catia Marzolini^{1,2,4} 

¹Division of Infectious Diseases and Hospital Epidemiology, Departments of Medicine and Clinical Research, University Hospital Basel, Basel, Switzerland

²Faculty of Medicine, University of Basel, Basel, Switzerland

³Certara UK Limited, Sheffield, UK

⁴Department of Molecular and Clinical Pharmacology, University of Liverpool, Liverpool, UK

Correspondence

Sara Bettonte, MS and Catia Marzolini, PharmD, PhD, Division of Infectious Diseases and Hospital Epidemiology, Departments of Medicine and Clinical Research, University Hospital Basel, Petersgraben 4, 4031 Basel, Switzerland.

Email: sara.bettonte@unibas.ch and catia.marzolini@usb.ch

Funding information

Schweizerischer Nationalfonds zur Förderung der Wissenschaftlichen Forschung, Grant/Award Number: 188504

Abstract

Aims: Intramuscular cabotegravir/rilpivirine (IM CAB/RPV) are metabolized by UGT1A1/CYP3A4. Efavirenz induces both enzymes; therefore, switching from an efavirenz-containing regimen to IM CAB/RPV could possibly result in suboptimal levels. Due to their long dosing interval, clinical studies with IM CAB/RPV are challenging. We used physiologically based pharmacokinetics (PBPK) modelling to simulate the switch from efavirenz to IM CAB/RPV.

Methods: First, we developed the drug models and verified the performance of the PBPK model to predict the pharmacokinetics of IM cabotegravir, IM rilpivirine and efavirenz by comparing the simulations against observed clinical data. Second, we verified the ability of the model to predict the effect of residual induction with observed data for the switch from efavirenz to dolutegravir or rilpivirine. Finally, we generated a cohort of 100 virtual individuals (20–50 years, 50% female, 18.5–30 kg/m²) to simulate IM CAB/RPV concentrations after discontinuing efavirenz in extensive and slow metabolizers of efavirenz.

Results: IM CAB concentrations were predicted to decrease by 11% (95% confidence interval 7–15%), 13% (6–21%) and 8% (0–18%) at day 1, 7 and 14 after efavirenz discontinuation. CAB concentrations were predicted to remain above the minimal efficacy threshold (i.e., 664 ng/mL) throughout the switch period both in extensive and slow metabolizers of efavirenz. Similarly, IM RPV concentrations were modestly decreased with the lowest reduction being 10% (6–14%) on day 7 post last efavirenz dose.

Conclusion: Our simulations indicate that switching from an efavirenz-containing regimen to IM CAB/RPV does not put at risk of having a time window with suboptimal drug levels.

KEYWORDS

drug–drug interaction; efavirenz; long-acting cabotegravir; long-acting rilpivirine; PBPK modelling, pharmacokinetics

This is an open access article under the terms of the [Creative Commons Attribution-NonCommercial-NoDerivs](https://creativecommons.org/licenses/by-nc-nd/4.0/) License, which permits use and distribution in any medium, provided the original work is properly cited, the use is non-commercial and no modifications or adaptations are made.

© 2023 The Authors. *British Journal of Clinical Pharmacology* published by John Wiley & Sons Ltd on behalf of British Pharmacological Society.

1 | INTRODUCTION

Cabotegravir and rilpivirine long-acting (LA) formulations have been licensed for the treatment of HIV infection in adults who are virologically suppressed. Cabotegravir and rilpivirine are administered intramuscularly (IM) in the gluteal area with an initial loading dose of 600 and 900 mg, respectively followed by a maintenance dose administered monthly (400 mg for cabotegravir and 600 mg for rilpivirine) or every other month (600 mg for cabotegravir, 900 mg for rilpivirine).¹ An oral lead-in phase of 30 days is used to ensure tolerability. However, since clinical trials and early real-world use have demonstrated good tolerability, the option is given to start with or without an oral lead-in phase.^{1,2} Cabotegravir is primarily metabolized by **uridine diphosphate-glucuronosyltransferase (UGT)1A1** while for rilpivirine the main elimination pathway is mediated by **cytochrome P450 (CYP) 3A4**.³ Thus, cabotegravir and rilpivirine are subject to drug–drug interactions (DDIs) notably with inducers of drug metabolizing enzymes, which can lead to subtherapeutic antiretroviral drug concentrations and the development of resistances. The label contraindicates the concurrent use of LA cabotegravir and rilpivirine with moderate or strong inducers.¹ It is currently unknown whether switching from an efavirenz-containing regimen or other antiretrovirals with moderate inducing properties (i.e., etravirine and nevirapine) directly to IM cabotegravir and rilpivirine could possibly result in a time window with suboptimal antiretroviral drug levels. Clinical DDIs studies are not available for LA cabotegravir and rilpivirine due to their long dosing interval which makes such studies difficult to conduct. Physiologically based pharmacokinetic (PBPK) modelling can overcome this limitation and be used to simulate clinically relevant and yet unstudied DDI scenarios. PBPK modelling has notably been applied to investigate the switch from efavirenz to dolutegravir (another integrase inhibitor substrate of UGT1A1 and CYP3A4) and to determine whether a dose adjustment of dolutegravir is needed in presence of residual induction by efavirenz.⁴

The main aim of this study was to simulate the initial IM cabotegravir and IM rilpivirine concentrations after stopping the moderate inducer efavirenz and to evaluate whether the concentrations remain above the effective range during the antiretroviral switch window. Furthermore, we simulated the pharmacokinetics of LA cabotegravir and rilpivirine in individuals with a slow **CYP2B6** metabolism phenotype which may result in higher concentrations of efavirenz and thereby impact the duration of the inducing effect after the drug discontinuation.⁵

2 | METHODS

We followed 3 steps to simulate the impact of the residual induction of efavirenz on LA cabotegravir and rilpivirine concentrations. First, we developed the drug models and verified the performance of the PBPK model to predict the pharmacokinetics of IM cabotegravir, IM rilpivirine (victim drugs) and efavirenz (perpetrator) by comparing the simulations against observed clinical data. Second, we verified the ability of the model to correctly predict the effect of residual induction with observed clinical data for the switch from efavirenz to

What is already known about this subject

- Clinical drug–drug interaction studies are difficult to conduct with long-acting drugs. It is unknown whether a dosing adjustment is required during the switch period from an efavirenz-containing regimen or other antiretrovirals with inducing properties to long-acting cabotegravir and rilpivirine. A physiologically based pharmacokinetic model can address this knowledge gap.

What this study adds

- Residual efavirenz concentrations were predicted to minimally reduce intramuscular cabotegravir and rilpivirine concentrations (<15%) 1, 7 and 14 days after discontinuing efavirenz. Therefore, switching from an efavirenz-containing regimen directly to intramuscular cabotegravir/rilpivirine would not put at risk of having a time window with suboptimal drug levels.

dolutegravir or rilpivirine. Finally, we applied the fully verified PBPK model to simulate the unstudied DDI scenario in extensive and poor CYP2B6 metabolizers.

2.1 | Drugs models development and verification

Our in-house PBPK model built in Matlab 2020a⁶ was implemented with an IM framework and verified against clinically observed data for LA cabotegravir and rilpivirine injected in the gluteal site as previously described.^{7,8} The drug models for cabotegravir and rilpivirine were built using the physicochemical and pharmacokinetic parameters listed in Table S1 and taking into account the following considerations. Cabotegravir reaches the peak concentration (C_{max}) 3 h after oral administration and 7 days after IM administration.⁹ The passive permeability is high³; however, the absolute oral bioavailability has not been measured.³ The fraction unbound in plasma is very low, while the blood-to-plasma ratio is 0.52.^{3,9} Cabotegravir is mainly metabolized by UGT1A1 and to a lesser extent by UGT1A9.³ The elimination half-life after oral administration is 41 h and 5.6–11.5 weeks after IM administration.³ Rilpivirine is a non-nucleoside reverse transcriptase inhibitor that reaches C_{max} 4 h after oral administration and 3–4 days after IM administration.³ The absolute oral bioavailability of rilpivirine has not been measured³; however, the measured bioavailability was 24–54% in preclinical species suggesting a high-first-pass metabolism.¹⁰ Additionally, the bioavailability is pH-dependent and is impacted by the presence of food.^{3,11,12} Rilpivirine is highly protein bound and has a blood-to-plasma ratio of 0.67.¹³ It is mainly

metabolized by CYP3A4 (fraction metabolized 75%)¹⁴ and exhibits a dose-proportionality increase in drug exposure in the dose range of 25–150 mg after oral administration.¹⁵ Finally, both LA IM drugs are characterized by flip-flop kinetics where the rate of absorption is slower than the rate of elimination therefore the elimination half-life is driven by the absorption.

The parameters used to develop efavirenz drug models for extensive and slow metabolizers are summarized in Table S1. Similarly to cabotegravir and rilpivirine, the efavirenz models were verified against clinical observed data.^{16–22} Efavirenz is a non-nucleoside reverse transcriptase inhibitor that reaches C_{max} 3–5 h after the first administration and after 10 days once steady-state has been reached.²³ Efavirenz has a good oral bioavailability,²⁴ binds highly to protein (mainly to albumin)²³ and is mainly metabolized by CYP2B6, CYP2A6 and UGT2B7.²⁵ Efavirenz is a moderate inducer of CYP3A4 and CYP2B6 and therefore induces also its own metabolism,²³ its terminal half-life is 52–76 h after 1 single dose and decreases to 40–55 h after multiple doses.²³ Dose-related increase in C_{max} and area under the concentration–time curve (AUC) are observed for doses up to 1600 mg.²³ The gene *CYP2B6* encoding the main enzyme responsible for efavirenz metabolism, displays a large number of single nucleotide polymorphisms (SNPs). Among them, the common SNP, characterized by a nucleotide change from G to T in position 516 in the coding region of *CYP2B6*, is characterized by a loss-of-function.⁵ Rodriguez-Novoa *et al.*, demonstrated that this SNP alters the catalytic activity rather than the protein expression.²¹ Thus, for the development of the efavirenz model in poor metabolizers, we modified the elimination rate of CYP2B6 but we did not change its abundance.

For all the compounds investigated, the models were considered verified if the predictions were within 2-fold of clinically observed data.^{26,27} Further information regarding the main parameters of the PBPK model, and the modelling strategies are found in the [Supporting Information](#).

2.2 | Model verification against switch clinical studies

The switch scenarios from efavirenz 600 mg to rilpivirine 25 mg (oral) or dolutegravir 50 mg for which observed clinical data are available were simulated using the same study design and study population characteristics (e.g., age range, proportion of female).^{28,29} The predictions were considered acceptable when the ratio between predicted vs. observed data was within 2-fold. The drug parameters used for the dolutegravir model development and for the simulation of the switch scenario are described in the Table S1. The reader should refer to the [Supporting Information](#) for a comprehensive description of the key dolutegravir absorption, distribution, metabolism and excretion properties and clinical behaviour (e.g., bioavailability, dose linearity) considered during the drug model development.

2.3 | Model application to unstudied DDI scenarios

A cohort of 100 virtual individuals (age 20–50 years, 50% female and body mass index 18.5–30 kg/m²) was generated by informing the model with equations describing the age-related changes of a healthy

TABLE 1 Ratio of predicted vs. observed (P/O) pharmacokinetic parameters for cabotegravir, rilpivirine, efavirenz (extensive metabolizer) and efavirenz (poor metabolizer) for the model validation.

Drug	Dosing regimen	Ratio P/O			Reference
		C_{max}	AUC	C_t	
Cabotegravir	30 mg PO, single dose	0.80	1.23	1.13	32–36
	30 mg PO, multiple dose	1.07	1.22	1.21	34,37–39
	800 mg IM, single dose	0.98	0.81	0.89	40
	800 mg IM, single dose, 400 mg IM, multiple dose	0.80	0.84	0.86	41
Rilpivirine	25 mg PO, single dose	0.79	1.02	-	28
	25 mg PO, multiple dose	0.88	1.00	0.90	28,38,42
	1200 mg IM, single dose	1.11	0.95	0.92	43
	25 mg PO, multiple dose, 900 mg IM every 8 weeks, multiple dose	-	-	0.63	44
Dolutegravir	50 mg PO, single dose	1.02	1.25	-	45,46
	50 mg PO, multiple dose	0.99	1.07	1.05	38,47,48
Efavirenz extensive metabolizer	600 mg PO, single dose	1.11	1.00	-	16,17
	600 mg PO, multiple dose	1.02	1.06	-	18
Efavirenz poor metabolizer	600 mg PO, single dose	0.99	1.55	-	19
	600 mg PO, multiple dose	-	0.72	0.71	20–22

Abbreviations: AUC, area under the curve; C_{max} , peak concentration; C_t , trough concentration; IM, intramuscular; PO, oral.

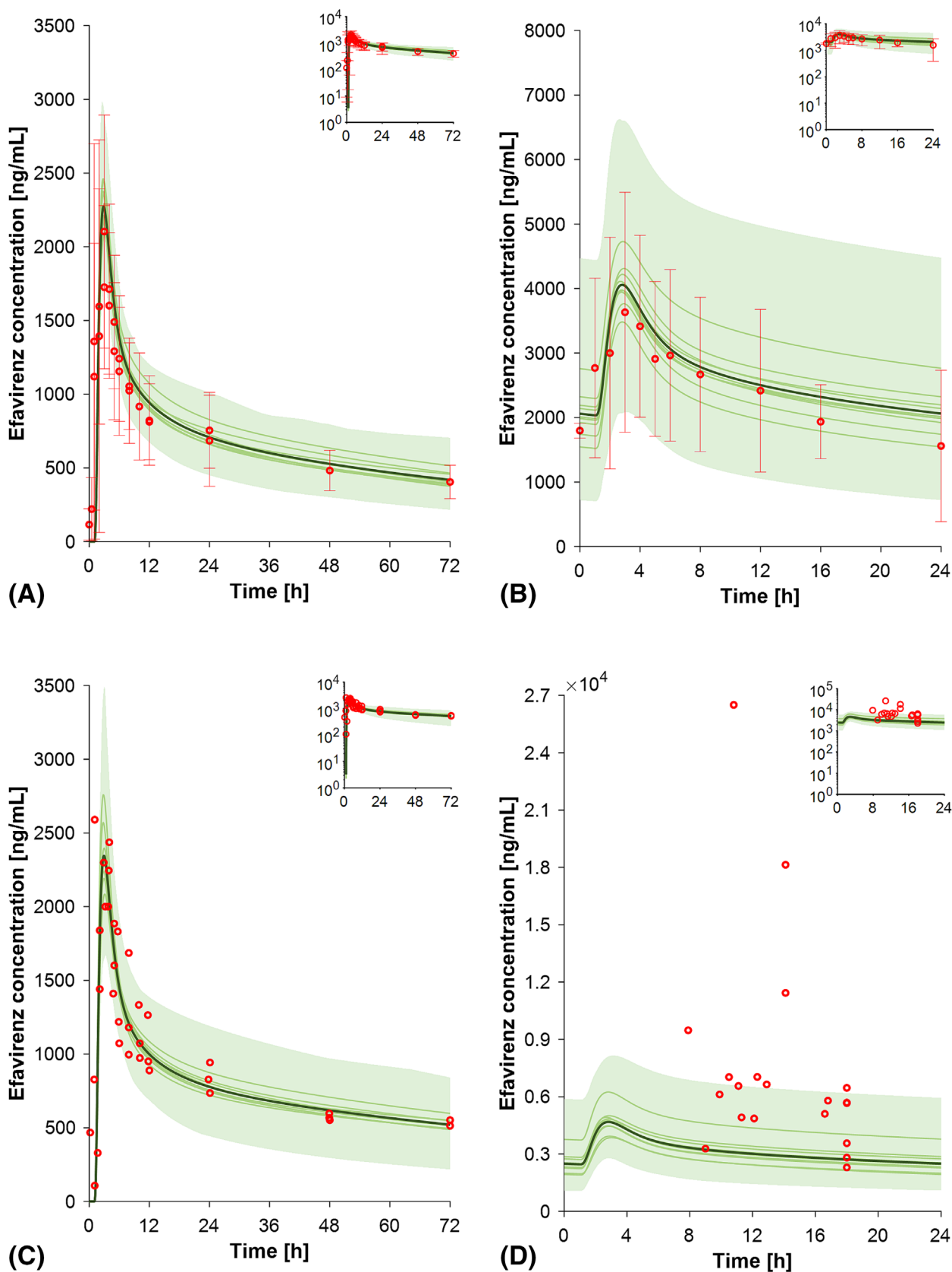


FIGURE 1 Predicted vs. observed concentration–time profiles for (A) efavirenz (extensive metabolizer) single-dose administration, (B) efavirenz (extensive metabolizer) at steady state, (C) efavirenz (slow metabolizer) single dose and (D) efavirenz (poor metabolizer) at steady state. The solid lines, the solid bold line and the shaded area represent the mean of each virtual trial, the mean of all trials and the 90% normal range of all virtual individuals. The red markers represent clinically observed data.

population (age 20–99 years).³⁰ The simulations were conducted by administering the first IM loading dose of cabotegravir (600 mg) and rilpivirine (900 mg) 12 h after stopping efavirenz (600 mg once daily at steady-state in extensive and slow metabolizer phenotypes). The effect of residual efavirenz induction was assessed by calculating the ratio of trough concentration (C_{τ}) and AUC to trough (AUC_{τ}) for IM cabotegravir and rilpivirine in presence and absence of residual efavirenz at various time points (i.e., 1, 7, 14 and 28 days after stopping efavirenz).

2.4 | Nomenclature of targets and ligands

Key protein targets and ligands in this article are hyperlinked to corresponding entries in <http://www.guidetopharmacology.org> and are permanently archived in the Concise Guide to PHARMACOLOGY 2019/2020.³¹

3 | RESULTS

3.1 | Drugs models development and verification

The drug models for IM cabotegravir, IM rilpivirine, efavirenz and dolutegravir were successfully developed and verified as the

predictions of the pharmacokinetic parameters were all within 2-fold of the clinically observed data. All the results are represented in Table 1. Additionally, Figure 1 shows the predicted vs. observed concentration profiles of efavirenz in extensive and poor metabolizers and Figure S1 the dolutegravir simulations for the verification of the drug model.

3.2 | Model verification against switch clinical studies

The model simulations were also in agreement with the clinically observed data measured during the switch from efavirenz to rilpivirine or dolutegravir.^{28,29} The ratio for the predicted vs. observed C_{τ} and AUC_{τ} for rilpivirine 25 mg (oral) after stopping efavirenz were within 1.5-fold at day 1, 14, 21 and 28 (Table 2, Figure 2). Similarly, the switch from efavirenz to dolutegravir 50 mg was predicted within 1.5-fold of the observed data (Table 2, Figure S2).²⁹

3.3 | Model application to unstudied DDI scenarios

Stopping efavirenz 12 h before initiating the administration of the first loading dose of LA cabotegravir (600 mg) was predicted to decrease

	Absence perpetrator Ratio P/O	After stopping perpetrator Ratio P/O	DDI ratio Ratio P/O	Reference
Rilpivirine—day 1 after stopping efavirenz				
$AUC_{0-\tau}$	1.13	1.08	0.95	28
C_{τ}^*	0.78	0.92	1.18	
Rilpivirine—day 14 after stopping efavirenz				
$AUC_{0-\tau}$	0.95	1.16	1.21	28
C_{τ}^*	0.98	1.27	1.29	
Rilpivirine—day 21 after stopping efavirenz				
$AUC_{0-\tau}$	0.97	1.13	1.16	28
C_{τ}^*	1.01	1.29	1.29	
Rilpivirine—day 28 after stopping efavirenz				
$AUC_{0-\tau}$	0.93	1.01	1.08	28
C_{τ}^*	1.01	1.18	1.16	
Dolutegravir—day 7 after stopping efavirenz				
$AUC_{0-\tau}$	-	-	-	29
C_{τ}^+	-	1.01	-	
Dolutegravir—day 14 after stopping efavirenz				
$AUC_{0-\tau}$	-	-	-	29
C_{τ}^+	-	1.41	-	
Dolutegravir—day 28 after stopping efavirenz				
$AUC_{0-\tau}$	-	-	-	29
C_{τ}^+	-	1.17	-	

TABLE 2 Ratio of predicted vs. observed (P/O) pharmacokinetic parameters for oral rilpivirine and dolutegravir after stopping the perpetrator drug efavirenz.

Abbreviations: $AUC_{0-\tau}$, area under the curve to trough [ng h/mL]; C_{τ}^* , concentration measured 24 h post-administration [ng/mL]; C_{τ}^+ , is the predose concentration [ng/mL]; DDI, drug–drug interaction.

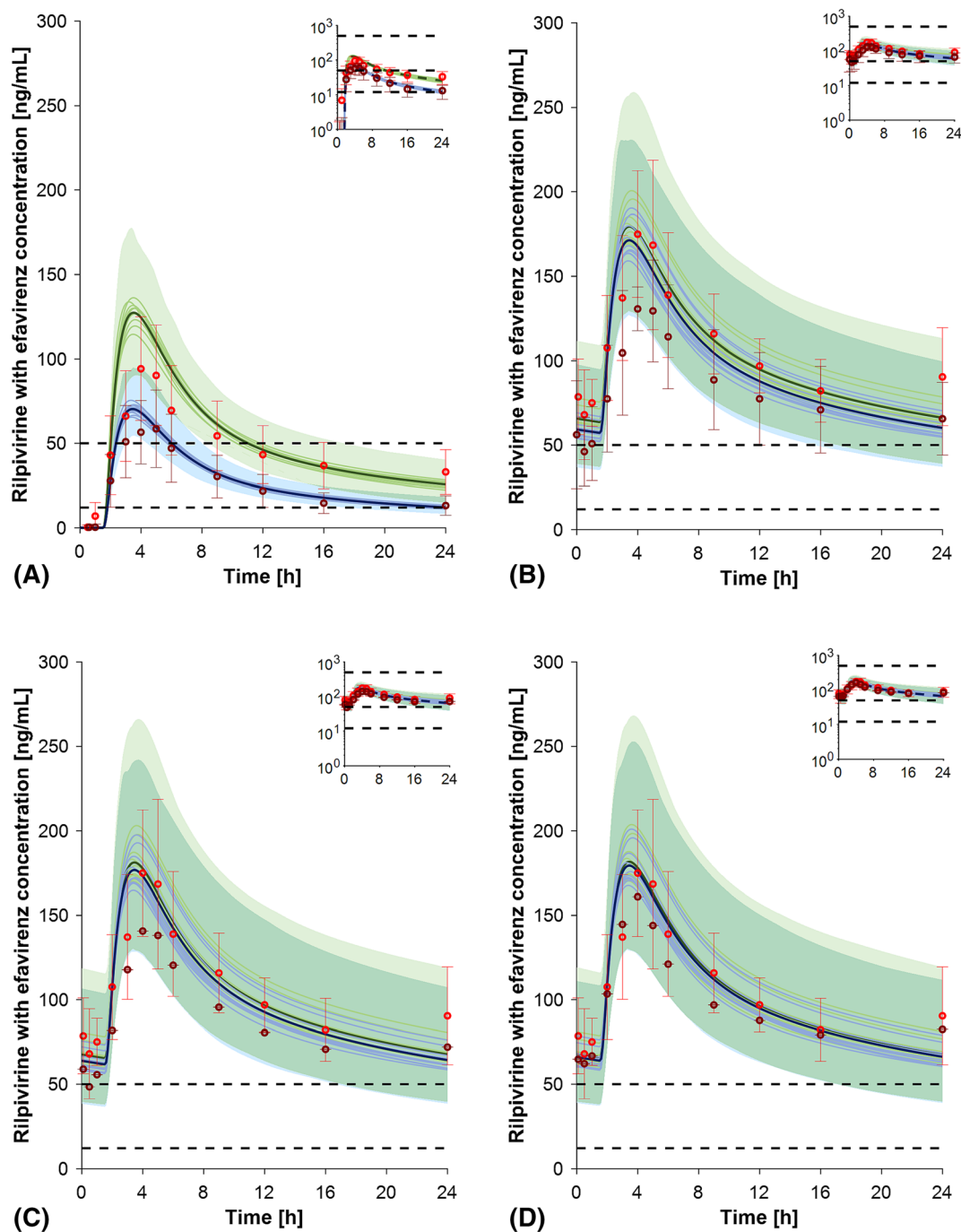


FIGURE 2 Predicted vs. observed concentration–time profiles for rilpivirine in the absence (green) and the presence (blue) of efavirenz inducing effect (A) at day 1, (B) at day 14, (C) at day 21 and (D) at day 28 after stopping the perpetrator. The solid lines, the solid bold line and the shaded area represent the mean of each virtual trial, the mean of all trials and the 90% normal range of all virtual individuals. The red and the dark markers represent clinically observed data for the control and drug–drug interaction scenarios, respectively. The dashed line represents the limit for QT prolongation risk (500 ng/mL), the minimal concentration for therapeutic response (50 ng/mL) and the protein-adjusted concentration required for 90% viral inhibition (12 ng/mL) for rilpivirine.

cabotegravir C_t by 11, 13, 8 and 2% on day 1, 7, 14 and 28 after stopping efavirenz. The corresponding decrease in AUC_t was 8, 15, 12 and 9%, respectively (Table 3). Importantly, the C_t was predicted to remain above the 4-fold protein-adjusted concentration required for 90% viral inhibition ($4 \times PA-IC_{90}$, i.e., 664 ng/mL)⁴⁹ throughout the

switch window both in extensive (Figure 3A) and slow efavirenz metabolizers (Figure 3C). The $4 \times PA-IC_{90}$ was selected as it has been associated with high treatment efficacy in phase 3 trials and with high protective efficacy in vaginal and rectal simian HIV challenge models.⁴⁹ By contrast, the residual inducing effect of efavirenz on the

TABLE 3 Pharmacokinetic parameters of the first intramuscular loading dose of LA cabotegravir and rilpivirine after stopping the perpetrator drug efavirenz in extensive genotype metabolizer individuals.

	Absence perpetrator Predicted	After stopping perpetrator Predicted	DDI ratio [95% CI] Predicted
Cabotegravir 600 mg, intramuscular—day 1 after stopping efavirenz 600 mg, oral			
C_{τ}	421 (20) [404–438]	373 (22) [357–390]	0.89 [0.85–0.93]
$AUC_{0-\tau}$	5419 (18) [5221–5617]	4968 (19) [4776–5160]	0.92 [0.88–0.95]
Cabotegravir 600 mg, intramuscular—day 7 after stopping efavirenz 600 mg, oral			
C_{τ}	1362 (41) [1241–1483]	1180 (40) [1080–1280]	0.87 [0.79–0.94]
$AUC_{0-\tau}$	151 919 (33) [141 467–162 370]	128 858 (34) [119 776–137 940]	0.85 [0.79–0.91]
Cabotegravir 600 mg, intramuscular—day 14 after stopping efavirenz 600 mg, oral			
C_{τ}	1251 (55) [1093–1409]	1153 (50) [1024–1283]	0.92 [0.82–1.03]
$AUC_{0-\tau}$	384 585 (42) [349 588–419 583]	336 968 (40) [307 770–366 167]	0.88 [0.80–0.95]
Cabotegravir 600 mg, intramuscular—day 28 after stopping efavirenz 600 mg, oral			
C_{τ}	962 (59) [837–1087]	939 (54) [823–1054]	0.98 [0.86–1.10]
$AUC_{0-\tau}$	739 518 (50) [657 209–821 827]	674 781 (47) [605 677–743 886]	0.91 [0.82–1.01]
Rilpivirine 900 mg, intramuscular—day 1 after stopping efavirenz 600 mg, oral			
C_{τ}	45 (17) [44–46]	42 (16) [41–44]	0.94 [0.91–0.98]
$AUC_{0-\tau}$	781 (15) [757–804]	740 (15) [718–763]	0.95 [0.92–0.98]
Rilpivirine 900 mg, intramuscular—day 7 after stopping efavirenz 600 mg, oral			
C_{τ}	79 (24) [75–83]	71 (21) [68–74]	0.90 [0.86–0.94]
$AUC_{0-\tau}$	11 190 (20) [10 741–11 639]	10 236 (19) [9859–10 614]	0.91 [0.88–0.95]
Rilpivirine 900 mg, intramuscular—day 14 after stopping efavirenz 600 mg, oral			
C_{τ}	45 (35) [42–48]	41 (29) [39–44]	0.92 [0.87–0.98]
$AUC_{0-\tau}$	21 523 (24) [20 496–22 550]	19 593 (21) [18 775–20 410]	0.91 [0.87–0.95]
Rilpivirine 900 mg, intramuscular—day 28 after stopping efavirenz 600 mg, oral			
C_{τ}	31 (35) [28–33]	30 (30) [28–32]	0.98 [0.90–1.03]
$AUC_{0-\tau}$	33 300 (28) [31 425–35 175]	30 748 (24) [29 270–32 226]	0.92 [0.88–0.97]

Note: The results are represented as geometric mean (CV) [95% CI].

Abbreviations: $AUC_{0-\tau}$, area under the curve to trough [ng h/mL]; CI, confidence interval; CV, coefficient of variance; C_{τ} , trough concentration [ng/mL]; DDI, drug-drug interaction.

first IM loading dose of rilpivirine (900 mg) was predicted to reduce the C_{τ} by 6, 10, 8 and 2% after 1, 7, 14, and 28 days with a similar effect on rilpivirine AUC_{τ} (reduction of 5, 9, 9 and 8% on day 1, 7, 14 and 28; Table 3). Twenty-eight days after stopping efavirenz, IM rilpivirine C_{τ} was 30 ng/mL, this value was below the minimal concentration associated with therapeutic response (i.e., 50 ng/mL)⁵⁰ regardless of the presence or absence of residual efavirenz concentrations both in extensive (Figure 3B) and slow metabolizers (Figure 3D). The simulated concentrations obtained are also in agreement with the clinical data measured in the FLAIR study after direct injection.²

4 | DISCUSSION

Although LA cabotegravir and rilpivirine represent an exciting advance for HIV care, several unanswered questions remain related to their use. Considering that LA cabotegravir and rilpivirine are only recommended in virologically suppressed people.¹ One of the current

knowledge gap was to determine whether a direct switch from a regimen including an antiretroviral drug with inducing properties (i.e., efavirenz, etravirine and nevirapine) to IM cabotegravir and rilpivirine allows to maintain sufficient drug exposure. A previous switch study with oral rilpivirine has indeed shown that residual efavirenz concentrations can reduce rilpivirine C_{τ} and AUC_{τ} , by 60 and 45% 1 day after stopping efavirenz. The reduction was still 30% for C_{τ} and 23% for AUC_{τ} 14 days after stopping efavirenz and mostly resolved after 21 days (i.e., AUC_{τ} lowered by <20%).²⁸ Our simulations suggest that residual efavirenz has a less pronounced effect on IM rilpivirine since both C_{τ} and AUC_{τ} were predicted to be reduced by $\leq 10\%$ during the switch period with the lowest reduction occurring at day 7. This difference is explained by the fact that rilpivirine has a high first-pass metabolism. Thus, the residual efavirenz inducing effect impacts both the intestinal and hepatic enzymes after oral administration and only the hepatic enzymes after IM administration. Similarly, residual efavirenz concentrations were predicted to cause a modest decrease in IM cabotegravir. Importantly, it should be highlighted that even if

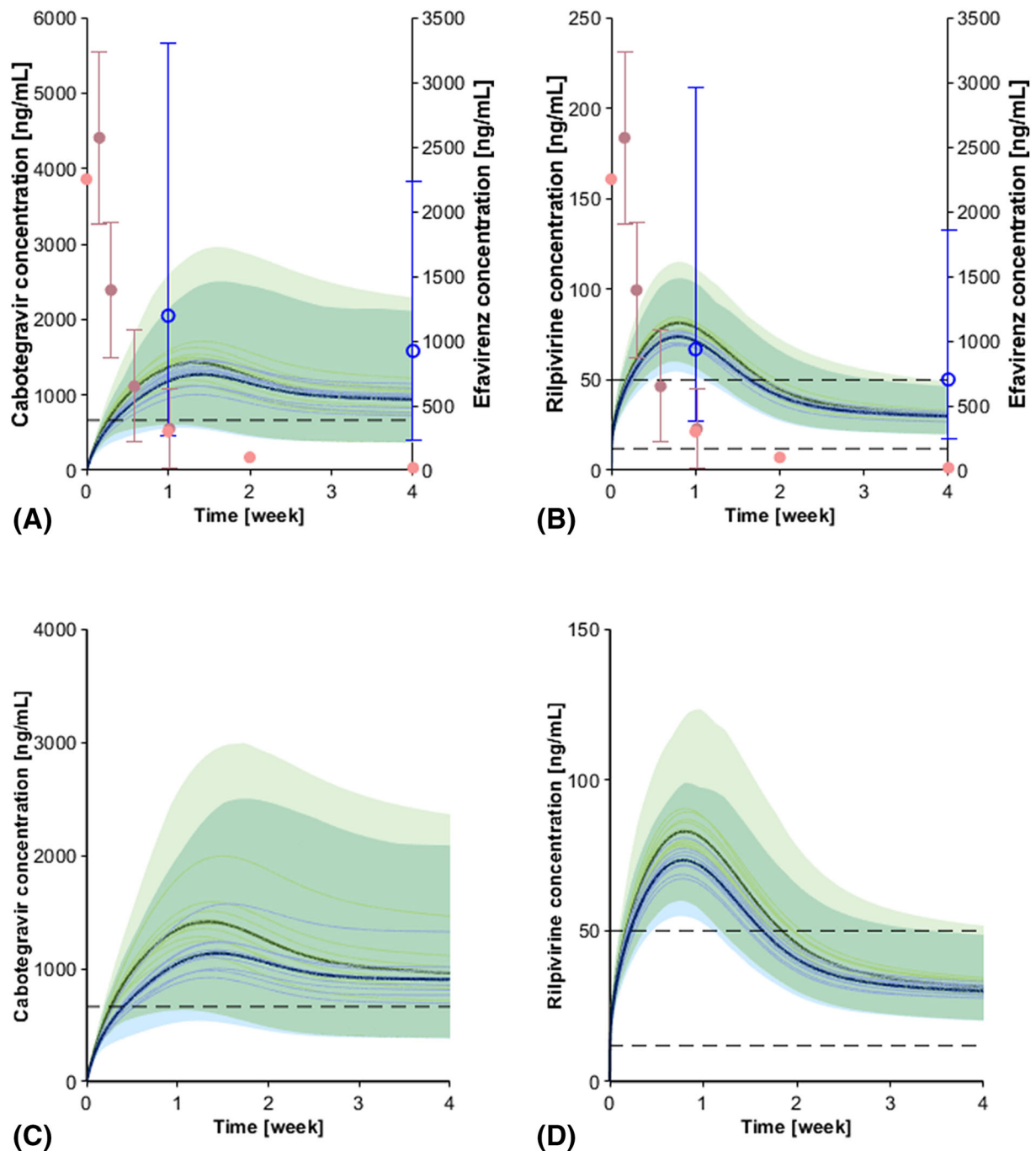


FIGURE 3 Concentration–time profiles for (A) cabotegravir 600 mg intramuscular loading dose, (B) rilpivirine 900 mg intramuscular loading dose in absence (green) and presence (blue) of efavirenz (extensive metabolizer) residual induction. Concentration–time profiles for (C) cabotegravir 600 mg intramuscular loading dose, (D) rilpivirine 900 mg intramuscular loading dose in absence (green) and presence (blue) of efavirenz (slow metabolizer) residual induction. The solid lines, the solid bold line and the shaded area represent the geometric mean of each virtual trial, the geometric mean of all trials and the 90% normal range of all virtual individuals. In (A), the dashed line represents the 4-fold protein-adjusted concentration required for 90% viral inhibition for cabotegravir (664 ng/mL).⁴⁹ In (B), the dashed lines represent the protein-adjusted concentration required for 90% viral inhibition for rilpivirine (12 ng/mL) and the minimal concentration for therapeutic response (50 ng/mL).⁵⁰ The lilac and the pink markers represent the mean measured efavirenz plasma decay concentration from Crauwels *et al.*²⁸ and Mills *et al.*,⁵¹ respectively. The open blue markers represent the median values measured from Orkin *et al.*² together with the 5th percentile and the 95th percentile for cabotegravir and rilpivirine LA after direct injection.

cabotegravir and rilpivirine concentrations reach their effective concentrations (i.e., 664 and 50 ng/mL, respectively) only 24 h after the initial IM loading dose; the concurrent residual efavirenz

concentrations are still well above the 1000 ng/mL effective threshold,⁵² thereby maintaining sufficient drug concentrations for the inhibition of viral replication.

The genetic variation in *CYP2B6* (i.e., G516T, *CYP2B6**6) has been shown to result in a longer efavirenz elimination half-life and higher concentrations in individuals homozygous for the T allele.⁵ Since the metabolic induction of efavirenz is concentration dependent, homozygous carriers of this variant have been shown to have more pronounced DDIs notably with etonogestrel.⁵³ Our simulations indicate that individuals with a slow efavirenz metabolizer genotype would have slightly lower cabotegravir and rilpivirine concentrations compared to extensive metabolizers however with no significant delay in reaching effective concentrations (Figure 3).

In conclusion, our simulations indicate that people on efavirenz-, etravirine- or nevirapine- based regimens with inducing properties could be directly switched to IM cabotegravir and rilpivirine without the risk of having a time window with suboptimal drug levels.

AUTHOR CONTRIBUTIONS

Sara Bettonte collected the data, ran the simulations, analysed the data and wrote the first draft of the manuscript. Mattia Berton contributed to the data analysis and writing of the manuscript. Felix Stader provided modelling input and supervised the data analysis. Manuel Battegay provided clinical input. Catia Marzolini designed the study, supervised the data analysis and obtained the funding. All authors contributed to the critical review and approval of the manuscript.

ACKNOWLEDGEMENTS

This work was supported by Swiss National Science Foundation [grant number 188504]. Open access funding provided by Universitat Basel.

CONFLICT OF INTEREST STATEMENT

C.M. received speaker honoraria from ViiV, MSD and Pfizer unrelated to this work. All other authors report no conflicts of interest.

DATA AVAILABILITY STATEMENT

The data that support the findings of this study are available upon request to the corresponding author.

ORCID

Sara Bettonte  <https://orcid.org/0000-0002-7532-7898>

Mattia Berton  <https://orcid.org/0000-0001-9450-2228>

Felix Stader  <https://orcid.org/0000-0002-4223-6754>

Manuel Battegay  <https://orcid.org/0000-0002-6638-3679>

Catia Marzolini  <https://orcid.org/0000-0002-2312-7050>

REFERENCES

- U.S. Food and Drug Administration. Cabenuva product label. Accessed May 2023, https://www.accessdata.fda.gov/drugsatfda_docs/label/2022/212888s005s006lbl.pdf
- Orkin C, Bernal Morell E, Tan DHS, et al. Initiation of long-acting cabotegravir plus rilpivirine as direct-to-injection or with an oral lead-in in adults with HIV-1 infection: week 124 results of the open-label phase 3 FLAIR study. *Lancet HIV*. 2021;8(11):e668-e678. doi:10.1016/S2352-3018(21)00184-3
- Hodge D, Back DJ, Gibbons S, Khoo SH, Marzolini C. Pharmacokinetics and drug-drug interactions of long-acting intramuscular cabotegravir and rilpivirine. *Clin Pharmacokinet*. 2021;60(7):835-853. doi:10.1007/s40262-021-01005-1
- Generaux G, Song I, Bowers G, Piscitelli S. A Mechanistic SimCYP Simulation Evaluating Dolutegravir and Efavirenz Pharmacokinetics Following a Switch From Once-daily Efavirenz to Once-daily Dolutegravir. Presented at: 15th international workshop on clinical pharmacology of HIV and hepatitis therapy; 2014. https://www.natap.org/2014/Pharm/Pharm_24.htm
- Ribaudo HJ, Haas DW, Tierney C, et al. Pharmacogenetics of plasma efavirenz exposure after treatment discontinuation: an adult AIDS Clinical Trials Group study. *Clin Infect Dis*. 2006;42(3):401-407. doi:10.1086/499364
- Stader F, Penny MA, Siccardi M, Marzolini C. A comprehensive framework for physiologically based pharmacokinetic modelling in Matlab (R). *CPT Pharmacometrics Syst Pharmacol*. 2019;8(7):444-459. doi:10.1002/psp4.12399
- Bettonte S, Berton M, Stader F, Battegay M, Marzolini C. Cabotegravir pharmacokinetics after oral and intramuscular administration using physiologically based pharmacokinetic modelling presented at: Population Approach Group Europe; 2022. <https://www.page-meeting.org/default.asp?abstract=10016>
- Bettonte S, Berton M, Stader F, Battegay M, Marzolini C. Management of drug-drug interactions between long-acting cabotegravir and rilpivirine and comedications with inducing properties: a modelling study. *Clin Infect Dis*. 2023;76(7):1225-1236. doi:10.1093/cid/ciac901
- U.S. Food and Drug Administration. Vocabria product label Accessed May 2023, https://www.accessdata.fda.gov/drugsatfda_docs/label/2021/212887s000lbl.pdf
- European Medicines Agency. Assessment report Edurant. Accessed May 2023, https://www.ema.europa.eu/en/documents/assessment-report/edurant-epar-public-assessment-report_en.pdf
- Crauwels HM, van Heeswijk RPG, Kestens D, et al. The pharmacokinetic (PK) interaction between omeprazole and TMC278, an investigational non-nucleoside reverse transcriptase inhibitor (NNRTI). *J Int AIDS Soc*. 2008;11(1):P239. doi:10.1186/1758-2652-11-S1-P239
- European Medicines Agency. Rekambys summary of product characteristics. Accessed May 2023, https://www.ema.europa.eu/en/documents/product-information/rekambys-epar-product-information_en.pdf
- Rajoli RK, Back DJ, Rannard S, et al. Physiologically based pharmacokinetic modelling to inform development of intramuscular long-acting nanoformulations for HIV. *Clin Pharmacokinet*. 2015;54(6):639-650. doi:10.1007/s40262-014-0227-1
- Center for drug evaluation and research. Clinical pharmacology and biopharmaceutics review(s). Addendum to Ondq biopharmaceutics review. Accessed May 2023, https://www.accessdata.fda.gov/drugsatfda_docs/nda/2011/202022Orig1s000ClinPharmR.pdf
- Crauwels H, van Heeswijk RP, Stevens M, et al. Clinical perspective on drug-drug interactions with the non-nucleoside reverse transcriptase inhibitor rilpivirine. *AIDS Rev*. 2013;15(2):87-101.
- Kharasch ED, Whittington D, Ensign D, et al. Mechanism of efavirenz influence on methadone pharmacokinetics and pharmacodynamics. *Clin Pharmacol Ther*. 2012;91(4):673-684. doi:10.1038/clpt.2011.276
- Cho DY, Shen JH, Lemler SM, et al. Rifampin enhances cytochrome P450 (CYP) 2B6-mediated efavirenz 8-hydroxylation in healthy volunteers. *Drug Metab Pharmacokinet*. 2016;31(2):107-116. doi:10.1016/j.dmpk.2015.07.002
- Villani P, Regazzi MB, Castelli F, et al. Pharmacokinetics of efavirenz (EFV) alone and in combination therapy with nelfinavir (NFV) in HIV-1 infected patients. *Br J Clin Pharmacol*. 1999;48(5):712-715. doi:10.1046/j.1365-2125.1999.00071.x

19. Xu C, Quinney SK, Guo Y, Hall SD, Li L, Desta Z. CYP2B6 pharmacogenetics-based in vitro-in vivo extrapolation of efavirenz clearance by physiologically based pharmacokinetic modeling. *Drug Metab Dispos.* 2013;41(12):2004-2011. doi:10.1124/dmd.113.051755
20. Siccardi M, Almond L, Schipani A, et al. Pharmacokinetic and pharmacodynamic analysis of efavirenz dose reduction using an in vitro-in vivo extrapolation model. *Clin Pharmacol Ther.* 2012;92(4):494-502. doi:10.1038/clpt.2012.61
21. Rodriguez-Novoa S, Barreiro P, Rendon A, Jimenez-Nacher I, Gonzalez-Lahoz J, Soriano V. Influence of 516G>T polymorphisms at the gene encoding the CYP450-2B6 isoenzyme on efavirenz plasma concentrations in HIV-infected subjects. *Clin Infect Dis.* 2005;40(9):1358-1361. doi:10.1086/429327
22. Haas DW, Smeaton LM, Shafer RW, et al. Pharmacogenetics of long-term responses to antiretroviral regimens containing Efavirenz and/or nelfinavir: an adult Aids clinical trials group study. *J Infect Dis.* 2005;192(11):1931-1942. doi:10.1086/497610
23. U.S. Food and Drug Administration. Sustiva product label Accessed May 2023, https://www.accessdata.fda.gov/drugsatfda_docs/label/2011/020972s038lbl.pdf
24. Vrouenraets SM, Wit FW, van Tongeren J, Lange JM. Efavirenz: a review. *Expert Opin Pharmacother.* 2007;8(6):851-871. doi:10.1517/14656566.8.6.851
25. Marzolini C, Rajoli R, Battegay M, Elzi L, Back D, Siccardi M. Physiologically based pharmacokinetic modeling to predict drug-drug interactions with Efavirenz involving simultaneous inducing and inhibitory effects on cytochromes. *Clin Pharmacokinet.* 2017;56(4):409-420. doi:10.1007/s40262-016-0447-7
26. Shebley M, Sandhu P, Emami Riedmaier A, et al. Physiologically based pharmacokinetic model qualification and reporting procedures for regulatory submissions: a consortium perspective. *Clin Pharmacol Ther.* 2018;104(1):88-110. doi:10.1002/cpt.1013
27. Abduljalil K, Cain T, Humphries H, Rostami-Hodjegan A. Deciding on success criteria for predictability of pharmacokinetic parameters from in vitro studies: an analysis based on in vivo observations. *Drug Metab Dispos.* 2014;42(9):1478-1484. doi:10.1124/dmd.114.058099
28. Crauwels H, Vingerhoets J, Ryan R, Witek J, Anderson D. Pharmacokinetic parameters of once-daily rilpivirine following administration of efavirenz in healthy subjects. *Antivir Ther.* 2012;17(3):439-446. doi:10.3851/IMP1959
29. de Wet J, DeJesus E, Sloan L, et al. Pharmacokinetics of dolutegravir after switching to abacavir/dolutegravir/lamivudine from an efavirenz-based regimen: a PK sub-study from STRIVING. presented at: 17th International Workshop on Clinical Pharmacology of HIV and Hepatitis Therapy; 2016. https://www.natap.org/2016/Pharm/Pharm_32.htm
30. Stader F, Siccardi M, Battegay M, Kinzig H, Penny MA, Marzolini C. Repository describing an aging population to inform physiologically based pharmacokinetic models considering anatomical, physiological, and biological age-dependent changes. *Clin Pharmacokinet.* 2019;58(4):483-501. doi:10.1007/s40262-018-0709-7
31. Alexander SPH, Fabbro D, Kelly E, et al. THE CONCISE GUIDE TO PHARMACOLOGY 2019/20: enzymes. *Br J Pharmacol.* 2019;176(S1):S297-S396. doi:10.1111/bph.14752
32. Shaik JSB, Ford SL, Lou Y, et al. A phase 1 study to evaluate the pharmacokinetics and safety of cabotegravir in patients with hepatic impairment and healthy matched controls. *Clin Pharmacol Drug Dev.* 2019;8(5):664-673. doi:10.1002/cpdd.655
33. Parasrampur R, Ford SL, Lou Y, et al. A phase I study to evaluate the pharmacokinetics and safety of cabotegravir in adults with severe renal impairment and healthy matched control participants. *Clin Pharmacol Drug Dev.* 2019;8(5):674-681. doi:10.1002/cpdd.664
34. Spreen W, Min S, Ford SL, et al. Pharmacokinetics, safety, and monotherapy antiviral activity of GSK1265744, an HIV integrase strand transfer inhibitor. *HIV Clin Trials.* 2013;14(5):192-203. doi:10.1310/hct1405-192
35. Patel P, Ford SL, Lou Y, et al. Effect of a high-fat meal on the pharmacokinetics of the HIV integrase inhibitor cabotegravir. *Clin Pharmacol Drug Dev.* 2019;8(4):443-448. doi:10.1002/cpdd.620
36. Ford SL, Sutton K, Lou Y, et al. Effect of rifampin on the single-dose pharmacokinetics of oral cabotegravir in healthy subjects. *Antimicrob Agents Chemother.* 2017;61(10):e00487-e00417. doi:10.1128/AAC.00487-17
37. Ford SL, Gould E, Chen S, et al. Effects of etravirine on the pharmacokinetics of the integrase inhibitor S/GSK1265744. *Antimicrob Agents Chemother.* 2013;57(1):277-280. doi:10.1128/AAC.01685-12
38. Ford SL, Gould E, Chen S, et al. Lack of pharmacokinetic interaction between rilpivirine and integrase inhibitors dolutegravir and GSK1265744. *Antimicrob Agents Chemother.* 2013;57(11):5472-5477. doi:10.1128/AAC.01235-13
39. Ford SL, Lou Y, Lewis N, et al. Effect of rifabutin on the pharmacokinetics of oral cabotegravir in healthy subjects. *Antivir Ther.* 2019;24(4):301-308. doi:10.3851/IMP3306
40. Spreen W, Ford SL, Chen S, et al. GSK1265744 pharmacokinetics in plasma and tissue after single-dose long-acting injectable administration in healthy subjects. *J Acquir Immune Defic Syndr.* 2014;67(5):481-486. doi:10.1097/QAI.0000000000000301
41. Spreen W, Williams P, Margolis D, et al. Pharmacokinetics, safety, and tolerability with repeat doses of GSK1265744 and rilpivirine (TMC278) long-acting nanosuspensions in healthy adults. *J Acquir Immune Defic Syndr.* 2014;67(5):487-492. doi:10.1097/QAI.0000000000000365
42. Dickinson L, Yapa HM, Jackson A, et al. Plasma tenofovir, emtricitabine, and rilpivirine and intracellular tenofovir diphosphate and emtricitabine triphosphate pharmacokinetics following drug intake cessation. *Antimicrob Agents Chemother.* 2015;59(10):6080-6086. doi:10.1128/AAC.01441-15
43. Jackson AG, Else LJ, Mesquita PM, et al. A compartmental pharmacokinetic evaluation of long-acting rilpivirine in HIV-negative volunteers for pre-exposure prophylaxis. *Clin Pharmacol Ther.* 2014;96(3):314-323. doi:10.1038/clpt.2014.118
44. Margolis DA, Gonzalez-Garcia J, Stellbrink HJ, et al. Long-acting intramuscular cabotegravir and rilpivirine in adults with HIV-1 infection (LATTE-2): 96-week results of a randomised, open-label, phase 2b, non-inferiority trial. *Lancet.* 2017;390(10101):1499-1510. doi:10.1016/S0140-6736(17)31917-7
45. Song I, Borland J, Chen S, et al. Effect of food on the pharmacokinetics of the integrase inhibitor dolutegravir. *Antimicrob Agents Chemother.* 2012;56(3):1627-1629. doi:10.1128/AAC.05739-11
46. Song IH, Borland J, Savina PM, et al. Pharmacokinetics of single-dose dolutegravir in HIV-seronegative subjects with moderate hepatic impairment compared to healthy matched controls. *Clin Pharmacol Drug Dev.* 2013;2(4):342-348. doi:10.1002/cpdd.55
47. Elliot ER, Wang X, Singh S, et al. Increased dolutegravir peak concentrations in people living with human immunodeficiency virus aged 60 and over, and analysis of sleep quality and cognition. *Clin Infect Dis.* 2019;68(1):87-95. doi:10.1093/cid/ciy426
48. Song I, Borland J, Min S, et al. Effects of etravirine alone and with ritonavir-boosted protease inhibitors on the pharmacokinetics of dolutegravir. *Antimicrob Agents Chemother.* 2011;55(7):3517-3521. doi:10.1128/AAC.00073-11
49. Landovitz RJ, Li S, Eron JJ Jr, et al. Tail-phase safety, tolerability, and pharmacokinetics of long-acting injectable cabotegravir in HIV-uninfected adults: a secondary analysis of the HPTN 077 trial. *Lancet HIV.* 2020;7(7):e472-e481. doi:10.1016/S2352-3018(20)30106-5
50. Aouri M, Barcelo C, Guidi M, et al. Population pharmacokinetics and pharmacogenetics analysis of rilpivirine in HIV-1-infected individuals. *Antimicrob Agents Chemother.* 2016;61(1):e00899-16. doi:10.1128/AAC.00899-16

51. Mills AM, Cohen C, Dejesus E, et al. Efficacy and safety 48 weeks after switching from efavirenz to rilpivirine using emtricitabine/tenofovir disoproxil fumarate-based single-tablet regimens. *HIV Clin Trials*. 2013;14(5): 216-223. doi:[10.1310/hct1405-216](https://doi.org/10.1310/hct1405-216)
52. Marzolini C, Telenti A, Decosterd LA, Greub G, Biollaz J, Buclin T. Efavirenz plasma levels can predict treatment failure and central nervous system side effects in HIV-1-infected patients. *Aids*. 2001;15(1):71-75. doi:[10.1097/00002030-200101050-00011](https://doi.org/10.1097/00002030-200101050-00011)
53. Neary M, Chappell CA, Scarsi KK, et al. Effect of patient genetics on etonogestrel pharmacokinetics when combined with efavirenz or nevirapine ART. *J Antimicrob Chemother*. 2019;74(10):3003-3010. doi:[10.1093/jac/dkz298](https://doi.org/10.1093/jac/dkz298)

SUPPORTING INFORMATION

Additional supporting information can be found online in the Supporting Information section at the end of this article.

How to cite this article: Bettonte S, Berton M, Stader F, Battegay M, Marzolini C. Intramuscular cabotegravir and rilpivirine concentrations after switching from efavirenz-containing regimen. *Br J Clin Pharmacol*. 2023;89(12): 3618-3628. doi:[10.1111/bcp.15867](https://doi.org/10.1111/bcp.15867)